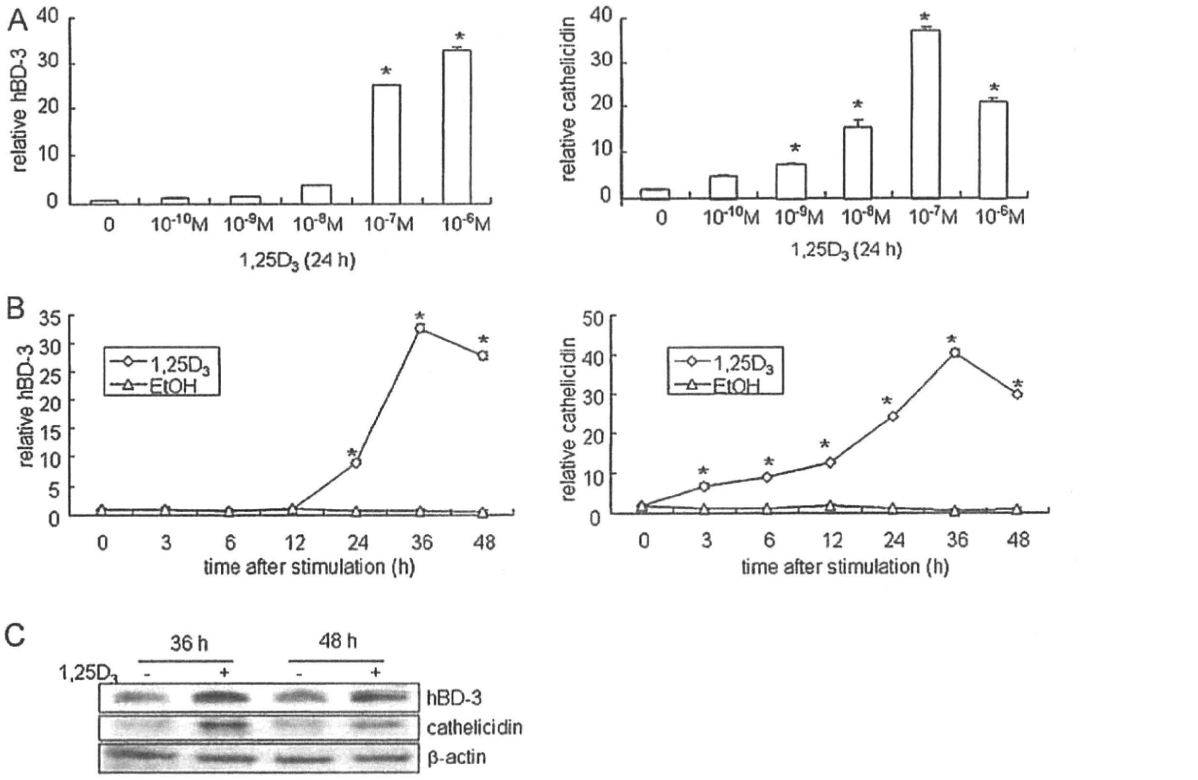

Fig. 1. 1,25D_3 stimulates hBD-3 and cathelicidin expression. (A) Subconfluent keratinocytes were incubated with different concentrations of 1,25D_3 for 24 h. Total RNA was collected, and real-time RT-PCR was performed to detect mRNA levels of hBD-3 and cathelicidin. (B) Keratinocytes were treated with 10^{-7} M 1,25D_3 and harvested after the indicated times. Total RNA was analyzed by real-time RT-PCR. (C) Keratinocytes were incubated with 10^{-7} M 1,25D_3 for 36 and 48 h, and the total extracts were subjected to Western blotting with antibodies against hBD-3, cathelicidin, and β-actin. The data represent at least three independent experiments. (*$p < 0.05$).

3. Results

3.1. Induction of antimicrobial peptides in human keratinocytes by 1,25D_3

We first investigated AMP expression in 1,25D_3-treated human keratinocytes. Increasing concentrations of 1,25D_3 produced a dose-dependent upregulation of hBD-3 and cathelicidin mRNA after 24 h of treatment; significant effects were observed at concentrations greater than 10^{-7} M (Fig. 1A). Stimulation of keratinocytes with 10^{-7} M 1,25D_3 resulted in robust induction of both hBD-3 and cathelicidin mRNA in a time-dependent manner, 1,25D_3 produced an approximately 30-fold increase in hBD-3 mRNA expression and a more than 40-fold increase in cathelicidin mRNA expression (Fig. 1B). Additionally, cathelicidin mRNA was significantly elevated beginning 3 h, whereas hBD-3 mRNA was significantly increased beginning 12 h after treatment (Fig. 1B). Similar to what was observed with mRNA expression, 1,25D_3 significantly upregulated hBD-3 and cathelicidin protein expression (Fig. 1C). However, 1,25D_3 did not significantly affect hBD-1 and hBD-2 expression (data not shown). The significant induction of cathelicidin in keratinocytes by 1,25D_3 is consistent with several previous reports [6,8]. We did not observe the rapid induction of hBD-2 by 1,25D_3, which conflicts with the data of Wang et al. [6], but is consistent with another report [9]. Notably, our data provide the first evidence for significant upregulation of hBD-3 by 1,25D_3 in keratinocytes.

3.2. PPARγ signal contributes to the induction of hBD-3 and cathelicidin by 1,25D_3

We next investigated if PPARγ signaling contributes to innate immunity in keratinocytes. Keratinocytes were transfected with a vector expressing wt-PPARγ, which resulted in abundant PPARγ protein expression (Fig. 2A) and stimulated PPARγ DNA binding activity as detected by EMSA analysis (Fig. 2B). Genetically enhanced PPARγ signaling produced a 7-fold increase in hBD-3 mRNA levels and a 5-fold increase in cathelicidin mRNA (Fig. 2C). Moreover, transfection with Ax-wt-PPARγ induced the phosphorylation of p38 (Fig. 2D), and increased AP-1 DNA binding activity in keratinocytes (Fig. 2E). Pretreatment with p38 inhibitor, SB203580, not only eliminated the wt-PPARγ-induced hBD-3 expression but also significantly reduced the mRNA induction of cathelicidin (Fig. 2F). These data suggest that PPARγ signal regulates AMP expression through activating p38 pathway in human keratinocytes.

Furthermore, the priming increase of PPARγ expression strongly upregulated the 1,25D_3-induced hBD-3 expression and sustained the 1,25D_3-mediated induction of cathelicidin (Fig. 3A). Next, we investigated if PPARγ activity is essential for 1,25D_3-induced AMP expression in keratinocytes. To examine the effects of PPARγ signaling on 1,25D_3 function, we transfected keratinocytes with dn-PPARγ, which specifically blocks PPARγ signaling [16]. Transfection with dn-PPARγ reduced 1,25D_3-induced cathelicidin mRNA expression by about 50%, and almost completely blocked the increases in hBD-3 mRNA (Fig. 3B). The dn-PPARγ also suppressed the 1,25D3-induced increases in hBD-3 and cathelicidin protein expression (Fig. 3C). These data indicate a potential role of PPARγ signaling in 1,25D3-stimulated innate immunity.

3.3. Transfection with dn-PPARγ does not affect binding of the DR-3 element

As the classical DR-3-type VDRE binding motif located in the cathelicidin promoter region [7] is responsible for 1,25D_3-

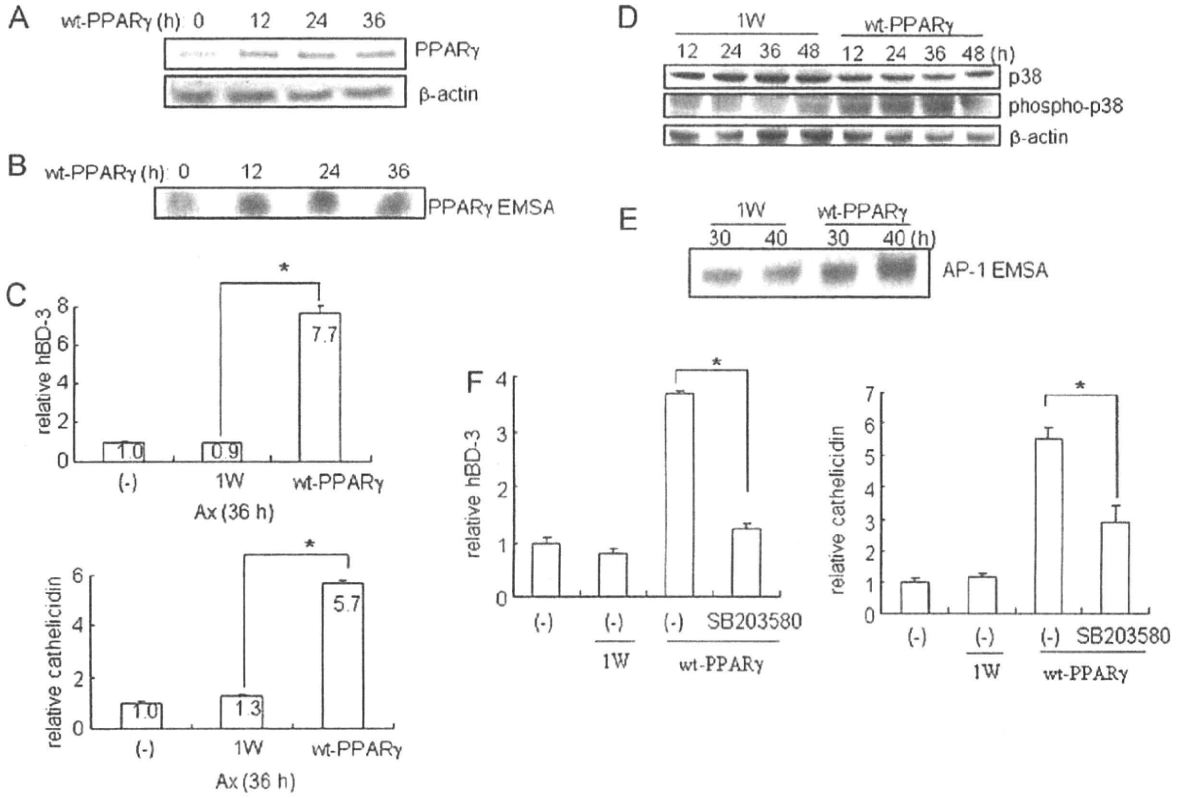

Fig. 2. wt-PPARγ induces the expression of hBD-3 and cathelicidin via activating p38 pathway. Keratinocytes were transfected with Ax-wt-PPARγ [multiplicity of infection (MOI) = 10] for 0, 12, 24, and 36 h. And cells were harvested for detection of PPARγ protein by Western blot analysis (A); and nuclear proteins were collected and incubated with biotin-labeled PPARγ probe, and EMSA was performed (B). (C) Keratinocytes were transfected with Ax-wt-PPARγ for 36 h. Total RNA was analyzed by real-time RT-PCR. Keratinocytes were transfected with Ax1W or Ax-wt-PPARγ for the indicated times, the total protein levels of p38 and phospho-p38 (D) and AP-1 DNA binding activity (E) were evaluated by western blotting and EMSA. (F) Keratinocytes were transfected with Ax-wt-PPARγ for 40 h in the presence or absence of 1 μM SB203580, the mRNA levels of hBD-3 and cathelicidin were detected using real-time RT-PCR. The data represent at least three independent experiments. (*$p < 0.05$).

mediated cathelicidin promoter activation and peptide expression in keratinocytes [6], we investigated whether PPARγ regulates cathelicidin transcription via facilitation of $1,25D_3$-induced protein binding to VDRE. Confirming a previous report [18], $1,25D_3$ rapidly induced VDR expression in keratinocytes (Fig. 4A), and stimulated the protein binding to the DR-3 element (Fig. 4B). But dn-PPARγ did not affect $1,25D_3$-induced VDR expression (Fig. 4A) and VDRE transactivation (Fig. 4B). Preincubation with unlabeled DNA blocked that protein binding, indicating that the probe used was specific (Fig. 4B). These data indicate that the VDRE in the cathelicidin promoter region is not involved in the regulation of cathelicidin induction by PPARγ in keratinocytes.

3.4. AP-1 and p38 activity contribute to PPARγ-mediated regulation of AMP induction by $1,25D_3$

As the AP-1 transcriptional binding motif has been detected in the promoter region of hBD-3 [15,19], we investigated if AP-1 activity is required for $1,25D_3$-mediated hBD-3 induction in keratinocytes. Three distinct MAPK signal pathways have been identified in mammalian cells: p38, ERK, and JNK, all of which contribute to AP-1 transcriptional activity by regulating the expression and phosphorylation of AP-1 subunits [20]. Treatment of keratinocytes with $1,25D_3$ resulted in the rapid and sustained phosphorylation of p38, ERK, and JNK (Fig. 5A), and increased AP-1 DNA-binding activity (Fig. 5D) [14]. Pretreatment with SB203580, PD98059, or SP600125, specific inhibitors of p38, ERK, and JNK, respectively, all strongly reduced hBD-3 mRNA induction in $1,25D_3$-treated keratinocytes (Fig. 5B). Despite the absence of an AP-1-binding motif in the promoter region of cathelicidin, SB203580 partially suppressed $1,25D_3$-mediated cathelicidin mRNA expression, while PD98059 and SP600125 presented no significant effect (Fig. 5B). No cytotoxic effects were produced by treatment with MAPK inhibitors. These data suggest that all three MAPK signaling pathways are critical for the transcription of hBD-3, whereas only the p38 pathway plays a role in the induction of cathelicidin mRNA in $1,25D_3$-treated keratinocytes.We next tested if PPARγ regulates $1,25D_3$-induced MAPK activation and AP-1 transactivation in keratinocytes. Transfection with dn-PPARγ significantly inhibited $1,25D_3$-induced p38 phosphorylation (Fig. 5C), but had no effect on ERK or JNK phosphorylation (data not shown). However, $1,25D_3$-induced AP-1 DNA-binding was almost completely blocked by dn-PPARγ (Fig. 5D). Moreover, dn-PPARγ suppressed the inducible total and nuclear expression of Fra1 and c-Fos (Fig. 5E and F), both of which participate in AP-1 formation and contribute to $1,25D_3$-induced AP-1 transactivation [21]. These data suggest that PPARγ regulates $1,25D_3$-induced AMPs production via p38 and AP-1 in human keratinocytes.

4. Discussion

The epidermal keratinocytes differentiate to form a physical barrier consisting of a multilayered epidermis and develop a chemical defense system based on the production of various AMPs [1,2]. We show here that $1,25D_3$ significantly induces hBD-3 and cathelicidin expression, but has no effect on hBD-1 and hBD-2 expression in cultured keratinocytes. $1,25D_3$ activates p38, ERK and JNK signaling pathways, increases c-Fos and Fra-1 expression

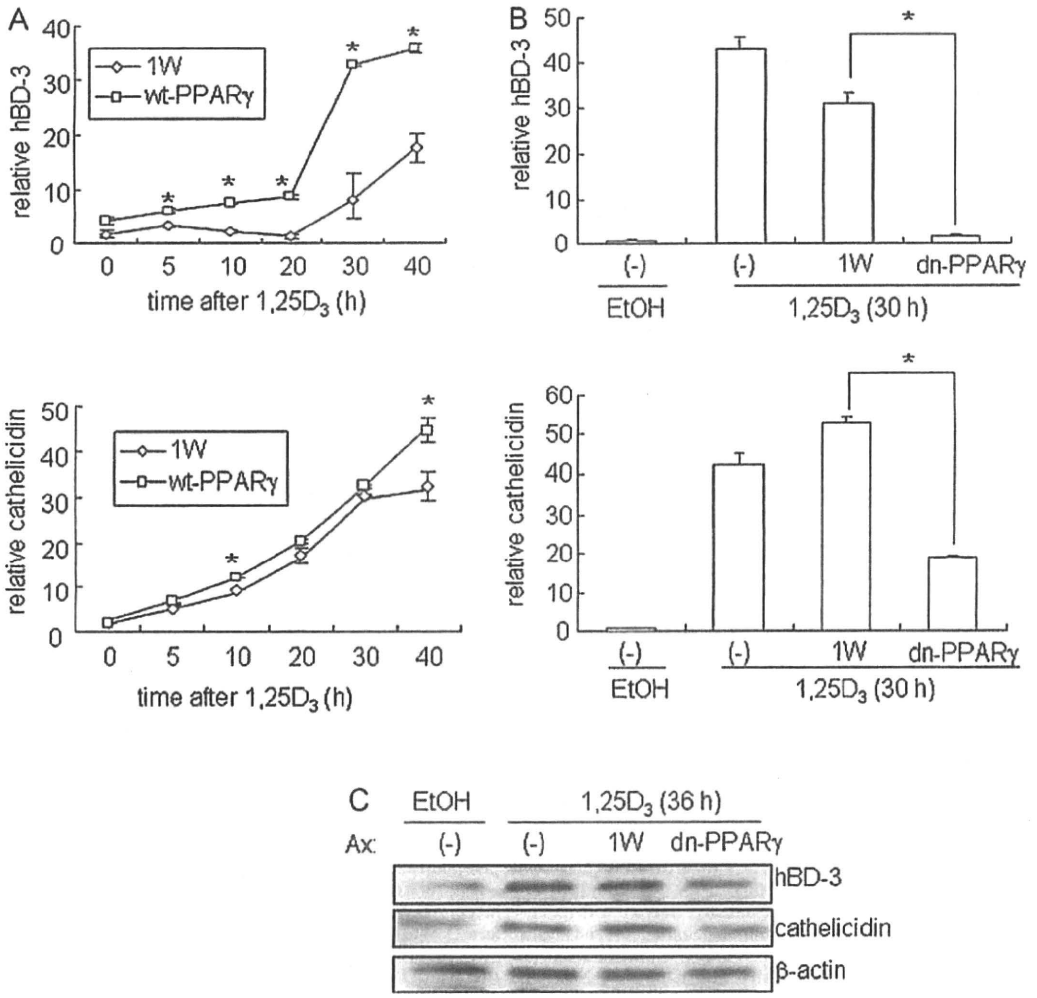

Fig. 3. dn-PPARγ interferes with the induction of hBD-3 and cathelicidin by $1,25D_3$. (A) Keratinocytes were transfected with Ax-wt-PPARγ for 12 h, then treated with $1,25D_3$ for the indicated times, the mRNA levels of hBD-3 and cathelicidin were detected using real-time RT-PCR. (B) Keratinocytes were transfected with Ax1W or Ax-dn-PPARγ (MOI = 10) for 24 h and then treated with $1,25D_3$. Total RNA was collected after 30 h, and the expression levels of hBD-3 and cathelicidin mRNA were detected using real-time RT-PCR. (C) Keratinocytes were transfected with Ax1W or Ax-dn-PPARγ and then incubated with $1,25D_3$ for 36 h, the protein levels of hBD-3 and cathelicidin were evaluated by Western blotting. The data represent at least three independent experiments. ($^*p < 0.05$).

and stimulates AP-1 transactivation in keratinocytes, which in turn induces hBD-3 transcription (Fig. 5). With respect to cathelicidin induction by $1,25D_3$, not only VDRE DNA-binding but also p38 activity is required (Fig. 5). Notably, our data provide the first evidence for the function of PPARγ in keratinocyte innate immunity. We show that PPARγ regulates AP-1 transactivation

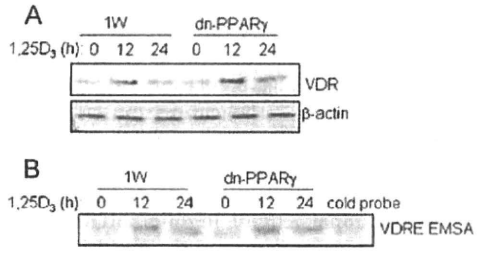

Fig. 4. dn-PPARγ has no effect on $1,25D_3$-mediated VDR expression and VDRE transactivation. Keratinocytes were transfected with Ax1W or Ax-dn-PPARγ then treated with $1,25D_3$ for the indicated times. VDR protein expression was detected by Western blot (A); and a biotin-labeled VDRE probe was incubated with the nuclear proteins, EMSA was performed (cold probe lane: an unlabeled probe was added before incubation with the biotin-labeled VDRE probe) (B). The data represent at least three independent experiments.

and p38 phosphorylation, which not only contributes to involucrin expression [14] but is also involved in the increased expression of hBD-3 and cathelicidin in $1,25D_3$-treated keratinocytes (Fig. 6). These data suggest a vital role for PPARγ in regulating the effects of $1,25D_3$ on keratinocyte differentiation and cell immunity.

The multiple signaling pathways are involved in the regulation of hBDs. hBD-2 expression is induced by NF-κB, AP-1, MAPK, and PKC, whereas the hBD-3 gene promoter has no discernible NF-κB binding elements but does contain transcriptional binding motifs for AP-1, IFN-γ response elements, and NF-IL-6 response elements [3]. We show here that all three AP-1 activating MAPK signaling pathways are necessary for $1,25D_3$-mediated hBD-3 induction, indicating a central role of AP-1 DNA binding in $1,25D_3$-mediated hBD-3 transcription in keratinocytes. We also demonstrate that PPARγ contributes to AP-1 transactivation by regulating $1,25D_3$-induced c-Fos and Fra1 expression, by which PPARγ signaling regulates hBD-3 expression in keratiocytes. Fos and Jun proteins participate in AP-1 formation, with various AP-1 homodimers or heterodimers carrying out cell-specific regulation of specific genes. Incubation of keratinocytes with $1,25D_3$ increased the expression of only c-Fos and Fra1, indicating that $1,25D_3$ activates specific AP-1 subtypes, which in turn may result in selective activation of AP-1 responsive genes depending on the composition of the AP-1 dimers

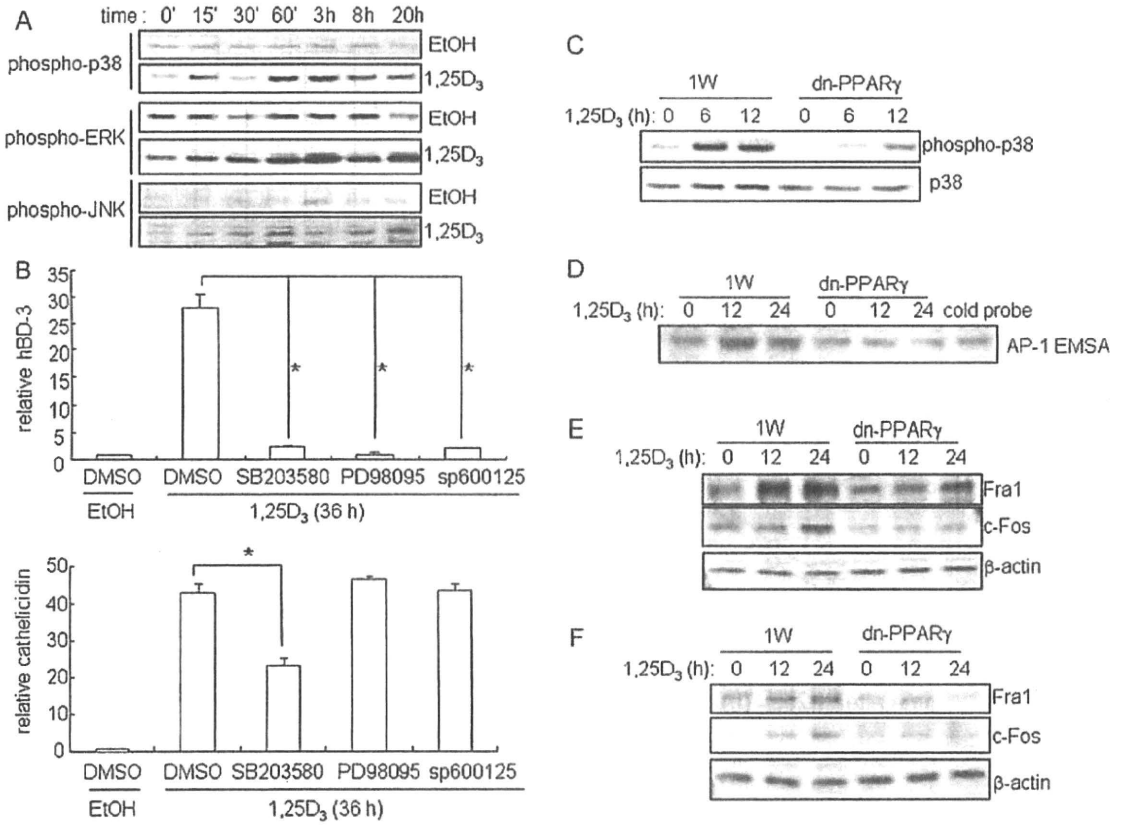

Fig. 5. Upregulation of AP-1 transactivation and p38 activity by $1,25D_3$ is inhibited by dn-PPARγ. (A) Keratinocytes were incubated with $1,25D_3$ for the indicated times, total lysates were collected, and Western blot analysis was performed to assess phopho-p38, phospho-ERK, and phospho-JNK protein levels. (B) Keratinocytes were preincubated with 1 μM SB203580, 30 μM PD98059, or 10 μM SP600125 for 1 h before $1,25D_3$ treatment. Total RNA was collected after 36 h, and the levels of hBD-3 and cathelicidin mRNA were measured using real-time PCR. Keratinocytes were infected with Ax-dn-PPARγ or Ax1W before the addition of $1,25D_3$. Cells were harvested after 6 h and 12 h, and p38 and phospho-p38 levels were evaluated by immunoblotting (C); and nuclear extracts were collected after 12 and 24 h, a biotin-labeled AP-1 probe was incubated with the nuclear proteins, and EMSA was performed (cold probe lane: an unlabeled probe was added before incubation with the biotin-labeled AP-1 probe) (D). Keratinocytes were infected with Ax-dn-PPARγ or Ax1W then treated with $1,25D_3$ for 12 and 24 h, after which the total cell lysates (E) and the nuclear extracts (F) were subjected to Western blotting to evaluate Fra1 and c-Fos protein levels. The data represent at least three independent experiments. ($^*p < 0.05$).

and promoter context. This feature may account for why $1,25D_3$ induces hBD-3 expression but not hBD-2 expression, even though AP-1 has been shown to regulate hBD-2 transcription [3].

Keratinocyte differentiation often contributes to hBD-3 expression [15,22]. Keratinocyte differentiation together with hBD-3 upregulation was induced not only by $1,25D_3$, as shown here, but also by other differentiation-inducing agents such as high calcium and retinoic acid (data not shown). These data suggest that keratinocyte differentiation, which activates AP-1, drives hBD-3 expression. We found that PPARγ signaling promotes the expression of both involucrin [14] and hBD-3, which is probably due to the ability of PPARγ to regulate keratinocyte differentiation and induce AP-1 transactivation.

Despite the absence of AP-1 motif on the promoter region of cathelicidin, the MEK–ERK pathway has been shown to be required for cathelicidin induction not only in butyrate-treated colon epithelial cells but also in $1,25D_3$-treated keratinocytes [9]. However, we found that p38 but not ERK phosphorylation contributed to cathelicidin induction by $1,25D_3$ in keratinocytes. This discrepancy may be attributable to the different culture conditions used. Although cell differentiation is not sufficient to induce cathelicidin expression [9], $1,25D_3$ and ASK1-mediated keratinocyte differentiation [15] regulate cathelicidin expression via the p38 pathway. Additionally, activation of PPARγ signaling, another differentiation-inducing event, contributes to cathelicidin expression through the regulation of p38 activity. Therefore, cell differentiation, activates p38 activity and induces cathelicidin expression at least in keratinocytes.

The expression of cathelicidin can be influenced by trans-acting enhancer element as well as by changes in transcript stability, and control may occur transcriptionally or posttranscriptionally, depending on cellular conditions. $1,25D_3$ induces cathelicidin expression in most $1,25D_3$-senstive human cells, including primary human keratinocytes, neutrophils, and monocytes [23], but not in colon epithelial cells, despite the expression of VDR in these cells [9]. $1,25D_3$ activates the cathelicidin promoter in colon epithelial cells but has no effect on mRNA and peptide expression. In contrast, despite the inability of butyrate to enhance cathelicidin promoter activity, butyrate elevates cathelicidin mRNA expression through a posttranscriptional regulation [9]. PPARγ activation most likely strengthens cathelicidin transcript stability by regulating p38 activity [24], thereby increasing cathelicidin mRNA expression, which needs further study.

Upon binding with VD3, VDR also recruits different coactivators to initiate transcriptional activity. In differentiated keratinocytes, recruitment of steroid receptor coactivators (SRCs) occurs in a cyclical manner and is required for optimal gene regulation [25]. SRC family members, such as SRC3, form complexes with VDR to recruit a number of histone acetyltransferases (HATs), which can increase HAT activity on chromatin and facilitate gene transcription [26,27]. SRC3 is strongly expressed in differentiated keratinocytes and aids in $1,25D_3$-mediated cathelicidin transcription

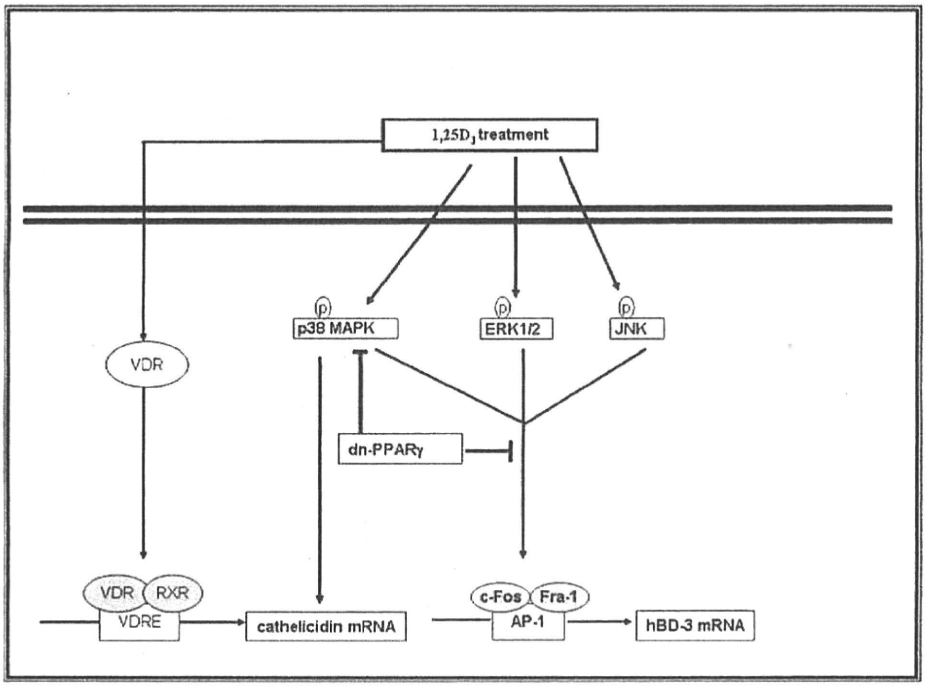

Fig. 6. A schematic model of a possible mechanism for the regulation of PPARγ on $1,25D_3$-mediated innate immune response. Treatment of keratinocytes with $1,25D_3$ activates p38, ERK and JNK MAP kinases and induces AP-1 transactivation, which in turn increases hBD-3 production. Upon the activation of VDRE, cathelicidin transcription is induced. The activation of p38 by $1,25D_3$ also contributes to the expression of cathelicidin. $1,25D_3$ stimulates PPARγ expression and signal activation, which is involved in $1,25D_3$-mediated hBD-3 and cathelicidin production by regulating AP-1 and p38 activity.

[25]. In addition to VDR, SRC family members also interact with other nuclear receptors such as RXR, LXR, and PPAR, to facilitate epidermal differentiation and cutaneous physiology [26,28]. SRC3 may be involved in the effects of PPARγ on cathelicidin expression, although this possibility requires further study.

AMPs have distinct regulatory systems, which supports their wide-ranging functional abilities. These peptides not only play an important role in the innate immune response, but also have inflammatory modulating and wound-healing capabilities [1–3,29]. $1,25D_3$ exerts multiple effects on AMP expression in keratinocytes, it not only regulates neutrophil gelatinase-associated lipocalin [6], but also induces cathelicidin and hBD-3 expression. Moreover, the effects of $1,25D_3$ on AMP expression are not limited to the VDR, as $1,25D_3$ also increases AMP expression via AP-1 and p38 pathway. Although PPARγ is best known as transcriptional regulator of lipid and glucose metabolism, evidence has also accumulated for its importance in skin homeostasis [10,12]. Here we provide the first evidence PPARγ activation facilitates the induction of hBD-3 and cathelicidin in keratinocytes following stimulation with $1,25D_3$ by regulating AP-1 and p38 activity, suggesting a potential role of PPARγ signaling in skin innate immunity.

Acknowledgments

We thank Teruko Tsuda and Eriko Tan for their excellent technical assistance. This work was supported by grants from the Ministries of Health, Labor, and Welfare and Education, Culture, Sports, Science and Technology, Japan.

References

[1] Schittek B, Paulmann M, Senyurek I, Steffen H. The role of antimicrobial peptides in human skin and in skin infectious diseases. Infect Disord Drug Targets 2008;8:135–43.
[2] Braff MH, Bardan A, Nizet V, Gallo RL. Cutaneous defense mechanisms by antimicrobial peptides. J Invest Dermatol 2005;125:9–13.
[3] Pazgier M, Hoover DM, Yang D, Lu W, Lubkowski J. Human beta-defensins. Cell Mol Life Sci 2006;63:1294–313.
[4] Kisich KO, Carspecken CW, Fieve S, Boguniewicz M, Leung DY. Defective killing of *Staphylococcus aureus* in atopic dermatitis is associated with reduced mobilization of human beta-defensin-3. J Allergy Clin Immunol 2008;122:62–8 [Epub 2008 Jun 5].
[5] Schauber J, Dorschner RA, Coda AB, Buchau AS, Liu PT, Kiken D, et al. Injury enhances TLR2 function and antimicrobial peptide expression through a vitamin D-dependent mechanism. J Clin Invest 2007;117:803–11 [Epub 2007 Feb 8].
[6] Wang TT, Nestel FP, Bourdeau V, Nagai Y, Wang Q, Liao J, et al. Cutting edge: 1,25-dihydroxyvitamin D3 is a direct inducer of antimicrobial peptide gene expression. J Immunol 2004;173:2909–12.
[7] Gombart AF, Borregaard N, Koeffler HP. Human cathelicidin antimicrobial peptide (CAMP) gene is a direct target of the vitamin D receptor and is strongly up-regulated in myeloid cells by 1,25-dihydroxyvitamin D3. FASEB J 2005;19:1067–77.
[8] Weber G, Heilborn JD, Chamorro Jimenez CI, Hammarsjo A, Torma H, Stahle M. Vitamin D induces the antimicrobial protein hCAP18 in human skin. J Invest Dermatol 2005;124:1080–2.
[9] Schauber J, Dorschner RA, Yamasaki K, Brouha B, Gallo RL. Control of the innate epithelial antimicrobial response is cell-type specific and dependent on relevant microenvironmental stimuli. Immunology 2006;118:509–19.
[10] Ellis CN, Varani J, Fisher GJ, Zeigler ME, Pershadsingh HA, Benson SC, et al. Differential expression of peroxisome proliferator-activated receptor subtypes during the differentiation of human keratinocytes. Arch Dermatol 2000;136:609–16.
[11] Demerjian M, Man MQ, Choi EH, Brown BE, Crumrine D, Chang S, et al. Topical treatment with thiazolidinediones, activators of peroxisome proliferator-activated receptor-gamma, normalizes epidermal homeostasis in a murine hyperproliferative disease model. Exp Dermatol 2006;15:154–60.
[12] Kuenzli S, Saurat JH, Ellis CN, Varani J, Fisher GJ, Zeigler ME, et al. Peroxisome proliferator-activated receptors in cutaneous biology. Br J Dermatol 2003;149:229–36.
[13] Dai X, Sayama K, Shirakata Y, Hanakawa Y, Yamasaki K, Tokumaru S, et al. STAT5a/PPARgamma pathway regulates involucrin expression in keratinocyte differentiation. J Invest Dermatol 2007;127:1728–35 [Epub 2007 Mar 1].
[14] Dai X, Sayama K, Shirakata Y, Tokumaru S, Yang L, Tohyama M, et al. PPAR gamma is an important transcription factor in 1 alpha,25-dihydroxyvitamin D3-induced involucrin expression. J Dermatol Sci 2008;50:53–60.
[15] Sayama K, Komatsuzawa H, Yamasaki K, Shirakata Y, Hanakawa Y, Ouhara K, et al. New mechanisms of skin innate immunity: ASK1-mediated keratinocyte differentiation regulates the expression of beta-defensins, LL37, and TLR2. Eur J Immunol 2005;35:1886–95.

[16] Gurnell M, Wentworth JM, Agostini M, Adams M, Collingwood TN, Provenzano C, et al. A dominant-negative peroxisome proliferator-activated receptor gamma (PPARgamma) mutant is a constitutive repressor and inhibits PPARgamma-mediated adipogenesis. J Biol Chem 2000;275:5754–9.
[17] Yahata Y, Shirakata Y, Tokumaru S, Yamasaki K, Sayama K, Hanakawa Y, et al. Nuclear translocation of phosphorylated STAT3 is essential for vascular endothelial growth factor-induced human dermal microvascular endothelial cell migration and tube formation. J Biol Chem 2003;278:40026–31 [Epub 2003 Jul 21].
[18] Jensen TJ, Henriksen LO, Solvsten H, Kragballe K. Inhibition of the 1,25-dihydroxyvitamin D3-induced increase in vitamin D receptor (VDR) levels and binding of VDR-retinoid X receptor (RXR) to a direct repeat (DR)-3 type response element by an RXR-specific ligand in human keratinocyte cultures. Biochem Pharmacol 1998;55:767–73.
[19] Menzies BE, Kenoyer A. Signal transduction and nuclear responses in *Staphylococcus aureus*-induced expression of human beta-defensin 3 in skin keratinocytes. Infect Immun 2006;74:6847–54 [Epub 2006 Sep 5].
[20] Whitmarsh AJ, Davis RJ. Transcription factor AP-1 regulation by mitogen-activated protein kinase signal transduction pathways. J Mol Med 1996;74:589–607.
[21] Johansen C, Kragballe K, Henningsen J, Westergaard M, Kristiansen K, Iversen L. 1alpha,25-dihydroxyvitamin D3 stimulates activator protein 1 DNA-binding activity by a phosphatidylinositol 3-kinase/Ras/MEK/extracellular signal regulated kinase 1/2 and c-Jun N-terminal kinase 1-dependent increase in c-Fos, Fra1, and c-Jun expression in human keratinocytes. J Invest Dermatol 2003;120:561–70.
[22] Abiko Y, Nishimura M, Kusano K, Yamazaki M, Arakawa T, Takuma T, et al. Upregulated expression of human beta defensin-1 and -3 mRNA during differentiation of keratinocyte immortalized cell lines, HaCaT and PHK16-0b. J Dermatol Sci 2003;31:225–8.
[23] Gombart AF, O'Kelly J, Saito T, Koeffler HP. Regulation of the CAMP gene by 1,25(OH)2D3 in various tissues. J Steroid Biochem Mol Biol 2007;103:552–7 [Epub 2006 Dec 23].
[24] Dai X, Yamasaki K, Shirakata Y, Sayama K, Hashimoto K. All-trans-retinoic acid induces interleukin-8 via the nuclear factor-kappaB and p38 mitogen-activated protein kinase pathways in normal human keratinocytes. J Invest Dermatol 2004;123:1078–85.
[25] Schauber J, Oda Y, Buchau AS, Yun QC, Steinmeyer A, Zugel U, et al. Histone acetylation in keratinocytes enables control of the expression of cathelicidin and CD14 by 1,25-dihydroxyvitamin D3. J Invest Dermatol 2008;128:816–24 [Epub 2007 Oct 18].
[26] Leo C, Chen JD. The SRC family of nuclear receptor coactivators. Gene 2000;245:1–11.
[27] Li B, Carey M, Workman JL. The role of chromatin during transcription. Cell 2007;128:707–19.
[28] Qi C, Zhu Y, Reddy JK. Peroxisome proliferator-activated receptors, coactivators, and downstream targets. Cell Biochem Biophys 2000;32:187–204.
[29] Tokumaru S, Sayama K, Shirakata Y, Komatsuzawa H, Ouhara K, Hanakawa Y, et al. Induction of keratinocyte migration via transactivation of the epidermal growth factor receptor by the antimicrobial peptide LL-37. J Immunol 2005;175:4662–8.

皮膚病診療：32(8)；895～898, 2010

◇薬疹——2010<臨床例>——⑬

Stevens-Johnson症候群と薬剤性過敏症症候群のオーバーラップした例

小田富美子*　藤山　幹子*　徳丸　晶*　村上　信司*　橋本　公二*

Key words
薬剤性過敏症症候群，Stevens-Johnson症候群，中毒性表皮壊死症，オーバーラップ

症例のポイント

- 薬剤性過敏症症候群(drug-induced hypersensitivity syndrome，以下，DIHS)は遅延性の薬疹で，発熱と多臓器症状を伴い，発症10日目以降にヒトヘルペスウイルス6(HHV-6)の再活性化を伴うことが特徴である．
- DIHSとStevens-Johnson症候群(以下，SJS)，中毒性表皮壊死症(toxic epidermal necrolysis，以下，TEN)は別のスペクトラムの薬疹と考えられていたが，近年DIHSとSJS，TENのオーバーラップと考えられる病態があることが明らかになってきた．
- SJSとDIHSのオーバーラップした1例を報告する．

症例　61歳，男．

初診　2008年5月．

家族歴　特記すべきことなし．

既往歴　2008年1月に脳出血．ゾニサミド，ファモチジンの内服を開始．

現病歴　2008年4月中旬より38℃台の発熱があり，セフジニルを内服したところ，5日後より全身に点状の紅斑が出現した．その翌日にセフジニルを中止し，さらに4日後よりプレドニゾロン(PSL)を10mg/日を処方された．軽快に伴い5月上旬より5mg/日に減量されていたが，発熱が続き，5日後より皮疹の増悪を認めたため，その翌日に当院に転院となった．

現症　体温38℃．体幹，四肢に非典型的な多形紅斑が多発し，前胸部，下肢では融合して紅斑局面を認めた(図1)．口唇にはびらんと血痂を認め，口腔内にもびらんとアフタがあり，一部には白苔をつけていた(図2)．鼻腔内にも痂皮を付着していた．両眼球結膜は軽度充血し，眼脂を認めたが，眼科的検査では結膜と角膜の上皮欠損は認めなかった．亀頭部の上皮剝離，鼠径部の表皮剝離も認めた(図3)．Nikolsky現象は陰性であった．また，耳前，顎下，腋窩，鼠径リンパ節は著明に腫脹していた．

臨床検査所見

血液検査(初診時)では，白血球 10,400/μl(好酸球10.0%，異型リンパ球7.0%出現)，GOT 84 IU/l，GPT 105 IU/l，LDH 314 IU/l，ALP 504 IU/l，γ-GTP 192 IU/lと血液障害，肝障害を認めた．CRPが7.88mg/dlと上昇していた．IgG 973mg/dlと低下はみられず，EBV EA-DR 10未満，EBV EBNA 10倍，EBV VCA IgG 160倍，CMV IgG 27.2(+)，CMV IgM 0.71(−)と既感染パターンを示した．

*Oda, Fumiko／Tohyama, Mikiko／Tokumaru, Sho(講師)／Murakami, Shinji(講師)／Hashimoto, Koji(教授)
愛媛大学医学部皮膚科学教室(〒791-0295 愛媛県東温市志津川)

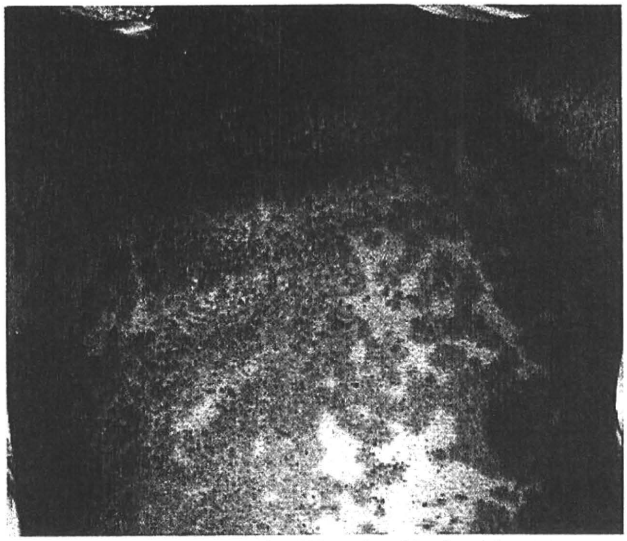

図1　体幹，四肢に非典型的な多形紅斑が多発する．

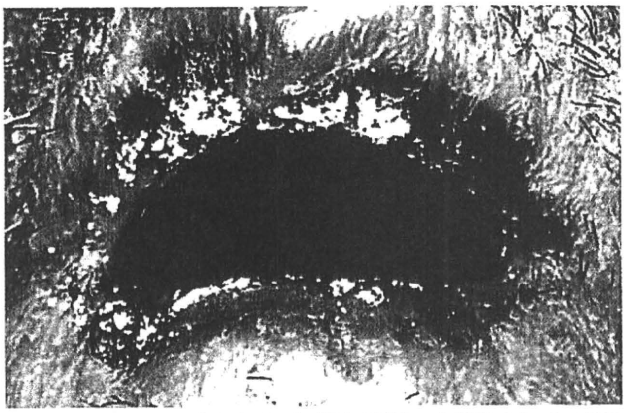

図2　口唇にはびらんと血痂を認め，口腔内にもびらんとアフタを形成する．

病理組織学的所見

左上腕の紅斑部から生検を施行した．表皮では液状変性を認め，真皮上層から真皮深層にかけて著明にリンパ球が浸潤していた．標本の一部では，ほぼ表皮全層性の表皮壊死と著明な液状変性，表皮下の裂隙も認めた．リンパ球の表皮内浸潤も顕著であった(図4)．

鑑別診断

発熱，紅斑やびらん，粘膜疹を呈する疾患を鑑別診断として考える．

EEM(多形滲出性紅斑)：一般に皮疹は2～3日かけて悪化し，2～3週間で消褪する．四肢伸側の関節部や顔面などに暗紅色，やや扁平な斑状丘疹状紅斑がみられ，次第に体幹に増数していくことも多い．皮膚病変部に水疱を形成する場合，口腔粘膜病変を高頻度に伴う．自験例は非典型多形紅斑であることより否定した．

麻疹：DIHS同様の播種状紅斑丘疹，顔面の潮紅，リンパ節腫大，高熱を認め鑑別がむずかしい．3～4日間，38℃前後の発熱とともにくしゃみ，鼻汁，眼脂，咳などのカタル症状をおこし，同時期にKoplik斑を認める．それに遅れて再度発熱し，カタル症状と発疹期を認める．その後，急激に3～4日で解熱する．自験例は麻疹の既往があることより否定した．

伝染性単核球症：発熱，咽頭痛，リンパ節腫脹が特徴的であり，DIHS様の播種状紅斑丘疹，肝機能障害や異型リンパ球の出現なども認められるが，自験例ではEBウイルス，サイトメガロウイルスとともに抗体価は既感染パターンであったため否定した．

診断確定

初診後の経過で，DIHSの診断基準の主要所見の，限られた薬剤投与後に生じた遅発性の紅斑，原因薬剤中止後2週間以上の遷延，38℃以上の発熱，肝機能障害，血液学的異常(白血球の増多，異型リンパ球の出現，好酸球増多)，リンパ節腫脹，HHV-6の再活性化のすべてを満たしており，典型的なDIHSと診断した[1]．

しかし，SJSの診断基準[2]である，皮膚粘膜移行部の重篤な粘膜病変，体表面積の10％未満のびらん，発熱と，副所見の非典型的な多形紅斑，表皮の壊死性変化を満たしSJSと診断できた．さらに，ほぼ全身に非典型的な多形紅斑を認めたこと，びらんを形成していない上腕部の皮膚生検で表皮のほぼ全層性の壊死が認められたこと，少量ではあったがPSLがすでに投与されていたことによる治療等の修飾により，表皮剝離が体表面積10％に達しなかった不全型TENとも考えられた[2]．

治療と経過

5月上旬の入院後(初診時)，内服薬をすべて中止した．PSLの増量を2日間行わず経過をみたところ，口唇と陰部のびらんは速やかに上皮化傾向を

認めた．しかし，39℃前後の高熱が続き，全身倦怠感も顕著であったため，　入院3日目よりPSL 80mgに増量した．その後は解熱傾向を示し，皮疹も軽快してきたが，その5日後ごろより再度39℃前後の高熱と高度の肝機能障害を認めた．このとき，　血清からHHV-6 DNA(69,000 copies/ml)，CMV DNA(56,000 copies/ml)が検出され，CMV抗原血症も陽性となった．高熱と肝機能障害はウイルス血症によるものと判断し，PSLを減量し，CMVに対してガンシクロビル投与を開始した．その後解熱し，肝機能も改善したが，5月下旬から再び血清中にCMV DNA(6,500 copies/ml)が検出され，一時的に四肢，体幹に5mm大までの褐色の丘疹が再燃した．5日後ごろよりガンシクロビルによると思われる汎血球減少が出現したため，その翌日に投与を中止したが，その後CMV DNAは陰性化した．汎血球減少と皮疹が改善したため，6月中旬よりPSLを5mg/日に減量し，10日後に転院した(**図5**)．

2008年6月中旬のDLST検査(S.I 181％以上で陽性)ではセフジニル 267％，ゾニサミド 96％，ファモチジン 148％でセフジニルのみ陽性であった．

図3　亀頭部，鼠径部の表皮剝離とびらん

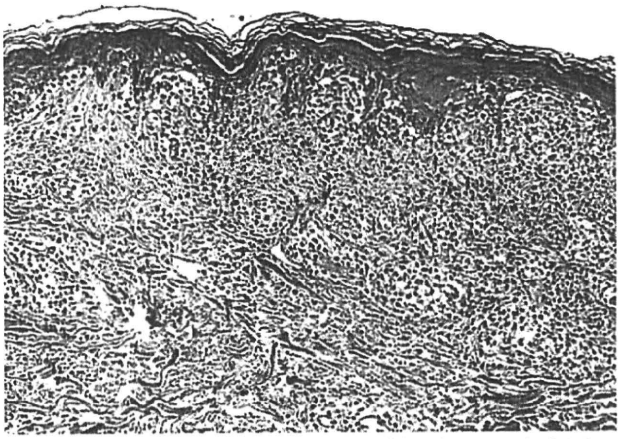

図4　標本中央ではほぼ表皮全層性の壊死と表皮下の裂隙を認める(H-E染色，10×20)．

考　按

自験例では臨床的に，口唇，口腔内，外陰粘膜にびらんと表皮剝離を認めることからまずSJSを疑った．病理組織検査でもSJSとして矛盾しない所見であり，SJSの診断基準を満たしているが，びらんを形成していない紅斑部で表皮の全層性壊死を認めたため，治療により修飾を受けた不全型TENとも考えられた．しかし，一方，臨床症状においてDIHSの原因薬剤の1つであるゾニサミド投与後に遅発性に紅斑を生じ，原因薬剤中止後も2週間以上遅延し，38℃以上の発熱，肝機能障害，血液学的異常(白血球の増多，異型リンパ球の出現，好酸球増多)，リンパ節腫脹，HHV-6の再活性化を認め，DIHSの診断基準を満たしている．

SJS/TENの診断は，体表の水疱，表皮剝離とびらんの面積，粘膜疹などの皮膚，粘膜の所見で診断される．一方，DIHSは，多臓器障害の存在と経過によって診断され，皮疹は紅斑としか定義されていない．そのため，皮膚所見をもってSJS/TENと診断され，　多臓器障害と臨床経過をもってDIHSと診断される症例が存在することは十分に考えられうる．

2005～2010年に，本邦ではDIHSとSJS，DIHSとTENのオーバーラップと考えられる症例が8例報告されている(**表**)[3~9]．7例はDIHSの原因薬剤であるゾニサミド，カルバマゼピン，アロプリノール，フェノバルビタールで発症しており，全例でHHV-6の抗体価の上昇を認め，DIHSの診断基準を満たしている．表皮剝離の面積から，5例がTENと診断されている[3~7]．SJSは自験例を含め3例である[8, 9]．粘膜皮膚移行部の障害は8例中6例で，口唇・口腔に認められ，外陰部の表皮剝離も認められているが，興味深いことに，眼の所見は充血が3例に認められたのみで，角膜障害を含めた重篤な障害は記載されていない．DIHSとSJS/TENの合

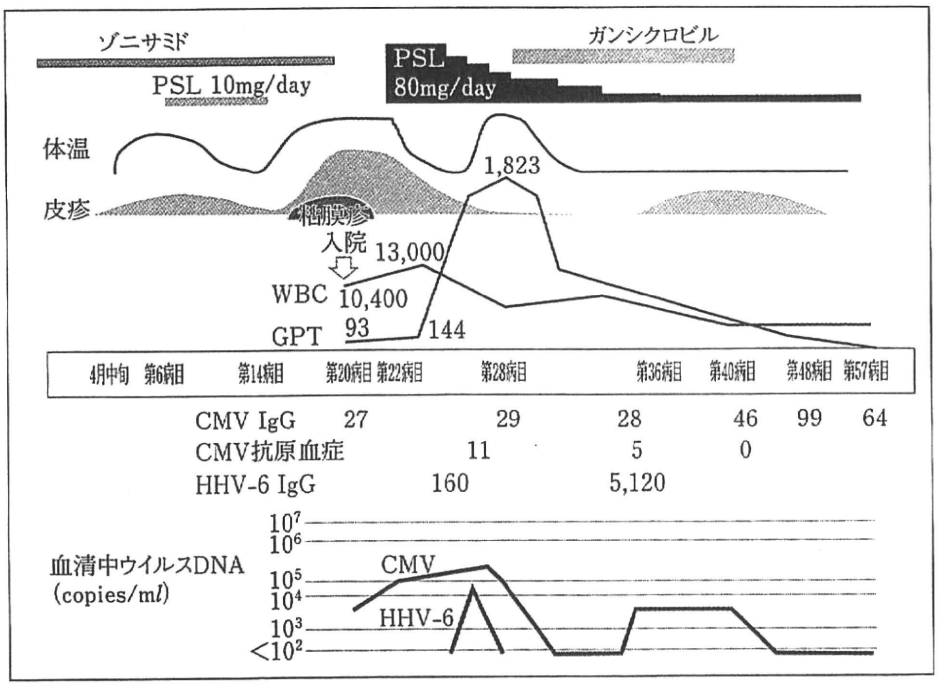

図5　経過図

表　DIHSとSJS/TENのオーバーラップ症例のまとめ

報告者	年齢・性	診断名	原因薬	粘膜疹			表皮剝離の範囲	表皮の全層性壊死
				眼	口	外陰		
広瀬ら[3]	17M	TEN	ゾニサミド	充血	＋	＋	全身	＋
金子ら[4]	41F	TEN	カルバマゼピン	－	－	－	臀部から下肢	＋
Terakiら[5]	71M	TEN	ゾニサミド	?	＋	?	体表面積の40%	＋
馬渕ら[6]	85F	TEN	アロプリノール	?	＋	?	全身	＋
久保田ら[7]	50F	TEN	フェノバルビター ル・セルトラリン	?	?	?	体表面積の40%	＋
狩野[8]	67M	SJS	フェノバルビタール	充血	＋	＋	陰茎, 陰嚢	－
西村ら[9]	27F	SJS	抗けいれん薬?	?	＋	?	体幹	?
自験例	61M	SJS	ゾニサミド	充血	＋	＋	鼠径部(2%)	＋

らは，DIHSとSJS/TENの皮膚病理組織を比較検討し，EEM型薬疹やEEM様皮疹より始まるDIHSでは，表皮のspongiosisが目立つ例が多く，interface changeは軽度であり，表皮角化細胞の壊死性変化も少数であり，SJSやTENの病理組織とは異なる性格をもつことを明らかにしている[7]．したがって，自験例のように皮膚病理組織像によって著明な表皮角化細胞の変性壊死を確認したときには，SJSあるいはTENがオーバーラップしたと判断する根拠となると思われる．

粘膜障害や表皮剝離を伴いSJS/TENが疑われる場合でも，DIHSの原因薬剤により遅発性に生じた薬疹であるときには，DIHSを合併している可能性も考え，治療，検査を進めていくことが必要である．

併では眼症状が軽度であることが特徴なのかもしれない．今後の症例の集積が必要であろう．

DIHSでも皮膚の水疱形成を認めることがあるが，病理組織学的には真皮乳頭層の強い浮腫に伴う水疱形成であり，表皮の壊死性変化はみられない[1]．そのため，皮膚生検はDIHSとSJS/TENの鑑別において有用であると考えられている．久保田

＜文　献＞
1) 橋本公二：日皮会誌　116：1575, 2006
2) 相原道子：日皮会誌　119：2157, 2009
3) 広瀬憲志ほか：西日皮膚　71：591, 2010
4) 金子　栄ほか：Visual Dermatology　4：1024, 2005
5) Teraki, Y. et al.：Arch Dermatol　144：232, 2008
6) 馬渕恵理子ほか：皮膚臨床　51：29, 2009
7) 久保田由美子ほか：日皮会誌　120：1015, 2010
8) 狩野葉子：Visual Dermatology　4：1022, 2005
9) 西村陽一ほか：日皮会誌　118：1546, 2008

THE JOURNAL OF DERMATOLOGY

doi: 10.1111/j.1346-8138.2009.00746.x

Journal of Dermatology 2010; **37**: 407–412

ORIGINAL ARTICLE

Erythema multiforme, Stevens–Johnson syndrome and toxic epidermal necrolysis: Frozen-section diagnosis

Hiroomi HOSAKA, Shinpei OHTOSHI, Tokio NAKADA, Masafumi IIJIMA

Department of Dermatology, Showa University School of Medicine, Tokyo, Japan

ABSTRACT

Stevens–Johnson syndrome (SJS) and toxic epidermal necrolysis (TEN) may be fatal. Although classified by body surface area skin detachment, initial stages of both may present with erythema multiforme (EM)-like lesions. To diagnose and predict disease activity adequately as early as possible for patients revealing EM-like lesions, we performed frozen-section diagnosis. Thirty-five patients clinically diagnosed as EM, SJS or TEN were biopsied to diagnose and predict disease progression within the initial-visit day. Half of a histological section taken from a lesion was snap-frozen and immediately cryostat-sectioned, acetone-fixed and stained with hematoxylin–eosin. Specimens were examined with light microscopy for presence of epidermal necrosis. A section from unaffected sites was also examined for 11 patients. Specimens were examined with light microscopy for presence of graft-versus-host reaction (GVHR)-like findings: apoptotic keratinocytes and satellite cell necrosis. Epidermal necrosis was seen in nine patients. Initial diagnosis of the nine was one of overlap SJS-TEN, four of SJS and four of EM, and final diagnosis of those was one of TEN, one of overlap SJS–TEN, four of SJS and three of EM. Dissociation between initial and final diagnosis was seen in three cases. GVHR-like findings in the epidermis were observed in two patients finally diagnosed as overlap SJS–TEN and TEN. Frozen sections are useful not only to make a diagnosis of erythema multiforme but to assess a potential to exhibit more aggressive clinical behaviors (SJS or TEN).

Key words: erythema multiforme, histopathology, rapid diagnosis, Stevens–Johnson syndrome, toxic epidermal necrolysis.

INTRODUCTION

Intraoperative rapid cytological diagnosis is useful for assessment of spread and activity of diseases (e.g. cancer) and selection of appropriate treatment. In dermatological diseases, Stevens–Johnson syndrome (SJS) and toxic epidermal necrolysis (TEN) have guarded prognosis: mortality rates were 6.3% and 21.6% in Japan, respectively,[1] and 13% and 39% from a retrospective study in Europe.[2] These are classified by skin detachment of body surface area: below 10% in SJS, between 10% and 30% in overlap SJS–TEN, and more than 30% in TEN with maculae.[3] In addition, in the retrospective study of severe erythema multiforme (EM) with skin and mucosal involvement, cutaneous lesions consisted of typical or raised atypical targets on the extremities and/or the face in EM major, while those lesions were flat atypical targets or purpuric maculae that were widespread or distributed on the trunk in SJS. In the initial stage, however, it is difficult to make a correct diagnosis because morphology suggests EM. Dermatologists, therefore, should diagnose and predict disease activity adequately as early as possible for patients revealing EM-like lesions.[4]

METHODS

Patients

The subjects were 35 patients (seven men and 28 women, with ages ranging 1–76 years [mean 47.4, standard deviation ± 17.7]) at our Department of

Correspondence: Tokio Nakada, M.D., Department of Dermatology, Showa University School of Medicine, 1-5-8 Hatanodai, Shinagawa-ku, Tokyo 142-8666 Japan. Email: tokio@med.showa-u.ac.jp

Received 13 July 2009; accepted 2 October 2009.

Table 1. Clinical and histopathological findings of 35 cases

No.	Age/sex	Initial diagnosis	Duration between onset and biopsy (days)	Systemic corticosteroid and IVIG before initial visit	Biopsy from cutaneous lesions			Biopsy from unaffected site		Final diagnosis
					Site	Lesion	Epidermal necrosis	Site	GVHR in the epidermis	
1	16/F	SJS	2	–	Right knee Left knee	Aypical target Purpuric maculae	+	Abdomen	+	TEN
2	61/F	EM major	0	–	Chest Right arm	Atypical target	–	Left arm	–	EM major
3	33/F	EM	7	Prednisolone 20 mg × 1 day	Right elbow	Purpuric maculae	–	NT	NT	EM
4	58/M	EM	2	–	Left femoral	Atypical target	–	NT	NT	EM
5	74/F	EM	6	–	Right forearm	Atypical target	–	NT	NT	EM
6	45/M	EM	4	Predonisolone 20 mg × 3 day	Right femoral	Atypical target (bullous)	–	NT	NT	EM
7	68/F	EM	2	–	Back	Typical target	–	NT	NT	EM
8	60/F	EM	1	–	Lumbar	Atypical target	+	NT	NT	EM
9	39/F	EM major	2	–	Right femoral	Atypical target	+	Right femoral	–	SJS
10	26/F	EM	1	–	Right femoral	Purpuric maculae	–	NT	NT	EM
11	53/F	SJS	3	–	Chest	Purpuric maculae	+	Right femoral	–	SJS
12	34/F	EM	1	–	Chest	Atypical target	–	NT	NT	EM
13	46/M	EM	6	Betamethasone 2 mg × 1 day + 4 mg × 1 day	Left femoral	Typical target	–	NT	NT	EM
14	39/F	SJS	3	Prednisolone 60 mg × 1 day Immunoglobulin 2.5 g × 1 day	Right femoral	Purpuric maculae	+	Right femoral	–	SJS
15	64/F	EM major	3	–	Back	Atypical target	–	Back	–	EM major
16	46/F	EM	4	–	Right arm	Atypical target (bullous)	–	NT	NT	EM
17	61/F	EM	20	Prednisolone 20 mg × 1 day	Abdomen Right arm	Purpuric maculae Atypical target (bullous)	+	NT	NT	EM
18	43/F	EM major	3	Betamethasone 0.75 mg × 1 day	Right forearm	Atypical target (bullous)	–	NT	NT	EM major
19	33/F	EM major	2	Betamethasone 1 mg × 1 day	Left femoral	Atypical target	–	Left femoral	–	EM major
20	35/F	EM major	2	–	Left arm	Atypical target	–	NT	NT	EM major
21	64/M	EM	3	Betamethasone 1.5 mg × 1 day	Right forearm	Atypical target	–	NT	NT	EM
22	39/F	EM major	4	Prednisolone 32 mg × 4 day (for neuro-Behçet's disease)	Back	Atypical target	–	NT	NT	EM major
23	72/F	EM	2	–	Right forearm	Typical target	–	NT	NT	EM
24	56/F	SJS–TEN	6	Hydrocortisone sodium phosphate 80 mg × 1 day	Right forearm Left wrist	Purpuric maculae	+	Right leg	+	SJS–TEN
25	34/F	EM	3	–	Back	Atypical target	–	NT	NT	EM
26	63/M	EM	5	Betamethasone 0.75 mg × 1 day	Right ankle Back	Atypical target (bullous) Atypical target	–	NT	NT	EM
27	76/F	EM	4	–	Left axilla Lumbar	Atypical target Purpuric maculae	–	NT	NT	EM

Table 1. *(Continued)*

No.	Age/sex	Initial diagnosis	Duration between onset and biopsy (days)	Systemic corticosteroid and IVIG before initial visit	Biopsy from cutaneous lesions			Biopsy from unaffected site			Final diagnosis
					Site	Lesion	Epidermal necrosis	Site	GVHR in the epidermis		
28	54/F	EM	5	–	Right wrist Neck	Bullous erythema Purpuric maculae	–	Left elbow	–		EM
29	21/M	SJS	3	Hydrocortisone sodium succinate 500 mg × 3 day	Left elbow	Typical target Atypical	+	Left arm	–		SJS
30	30/F	SJS?	3	–	Right hand	Purpuric maculae	–	Right hand	–		EM major
31	55/F	EM major	11	Hydrocortisone sodium succinate 300 mg × 3 day + 800 mg × 1 day	Left hand	Atypical target	+	NT	NT		EM major
32	1/F	EM	2	–	Right femoral	Atypical target	–	NT	NT		EM
33	32/F	EM major	7	–	Left femoral	Atypical target	–	NT	NT		EM major
34	61/M	EM	3	–	Abdomen	Typical target	–	NT	NT		EM
35	71/F	EM major	3	Prednisolone 10 mg × 1 day	Right femoral	Atypical target	–	NT	NT		EM major

EM, erythema multiforme; SJS, Stevens-Johnson syndrome; SJS–TEN, overlap SJS–TEN; TEN, toxic epidermal necrolysis; NT, not tested; IVIG, i.v. immunoglobulin; GVHR, graft-versus-host reaction.

Dermatology, tested from March 2003 to February 2008. Except for cases 4 and 17, all were inpatients. Clinical diagnoses were preformed on the basis of the classification by Bastuji-Garin *et al.* and the retrospective study by Assier *et al.* described above on the initial-visit day by dermatologists in the Department. These were EM (29 patients including 10 EM major), SJS (five patients) and overlap SJS–TEN (one patient) (Table 1). Staphylococcal scalded skin syndrome was excluded by clinical symptoms: presence of mucous lesions and negative Nicolsky's sign in uninvolved skin.

MATERIALS AND METHODS

Specimens were obtained from cutaneous lesions: typical target lesions, atypical target lesions and purpuric macules were selected in that order. These were either processed for light microscopy, or frozen in liquid nitrogen for rapid histological diagnosis. For routine histology, half of the specimen was fixed with 10% formalin. The other half of the specimen was immediately snap-frozen, cryostat-sectioned at 4-mm intervals, acetone-fixed and then stained with hematoxylin–eosin for immediate histological diagnosis. Specimens taken from unaffected sites were also examined for 11 patients initially diagnosed as one of SJS–TEN, five of SJS, four of EM major and one of EM on the basis of moderate or severe cutaneous lesions. Specimens were examined with light microscopy to ascertain presence of necrosis and graft-versus-host reaction (GVHR)-like findings: apoptotic keratinocytes and satellite cell necrosis in the epidermis.

RESULTS

In the rapid histological diagnosis, epidermal necrosis was seen in nine of the 35 patients (25.7%, Table 1). Initial diagnosis of the nine was one of SJS–TEN, four of SJS and four of EM, and final diagnosis of these was one of TEN, one of SJS–TEN, four of SJS and three of EM. Dissociation between initial and final diagnosis was seen in three cases (cases 1, 9 and 30) (Table 1). GVHR-like findings in unaffected sites were seen in two patients (cases 1, 24): both were diagnosed as SJS or SJS–TEN at the initial-visit day, and as TEN and SJS–TEN finally (Table 1, Fig. 1). Figure 1

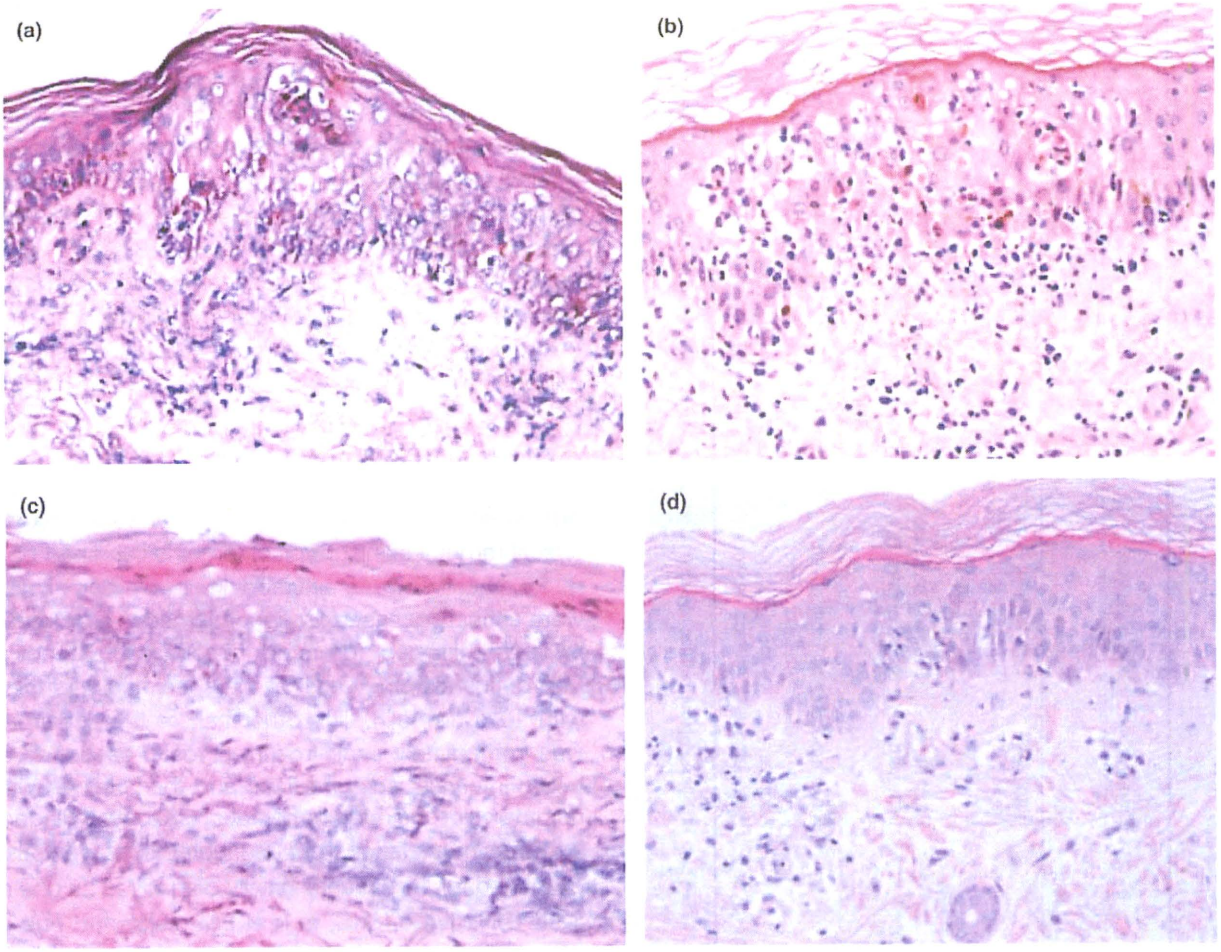

Figure 1. Histopathological findings of case 24. (a) Frozen sections from a lesion. (b) Permanent specimen from a lesion. Exocytosis of lymphocytes and epidermal necrosis are noted. (c) Frozen section of unaffected skin. (d) Permanent specimen from unaffected skin. Apoptotic keratinocytes and exocytosis of lymphocytes are noted (hematoxylin–eosin, original magnification ×400).

shows histopathological findings of case 24: both frozen and permanent specimens revealed overt epidermal necrosis from a lesion and mild GVHR-like findings in the epidermis from unaffected skin. In case 29, both frozen and permanent specimens showed epidermal damage from a lesion while no overt findings from unaffected skin (Fig. 2).

The limitation of this study was that it comprised a small group.

DISCUSSION

The relationship between EM and SJS is subjective: some cases present clinical difficulty in differentiating EM major and SJS. Histopathologically, EM show a vacuolar form of interface dermatitis whereas SJS and TEN reveal more epidermal necrosis, less dermal inflammation and exocytosis.[5] Cote *et al.*[6] suggested that histopathological findings are helpful: EM major shows less epidermal necrosis, more dermal infiltration and more exocytosis than SJS. Our results concur with their suggestion because epidermal necrosis was observed in all six patients finally diagnosed as SJS, overlap SJS–TEN or TEN while only 10.3% of EM (Table 2). Epidermal necrosis was observed from 1–20 days after onset of rash, and it was seen despite previous treatment with systemic corticosteroid and immunoglobulin (cases 14, 17, 24, 29, 31) (Table 1).

Stevens–Johnson syndrome and TEN are considered as disorders of different severity within the same

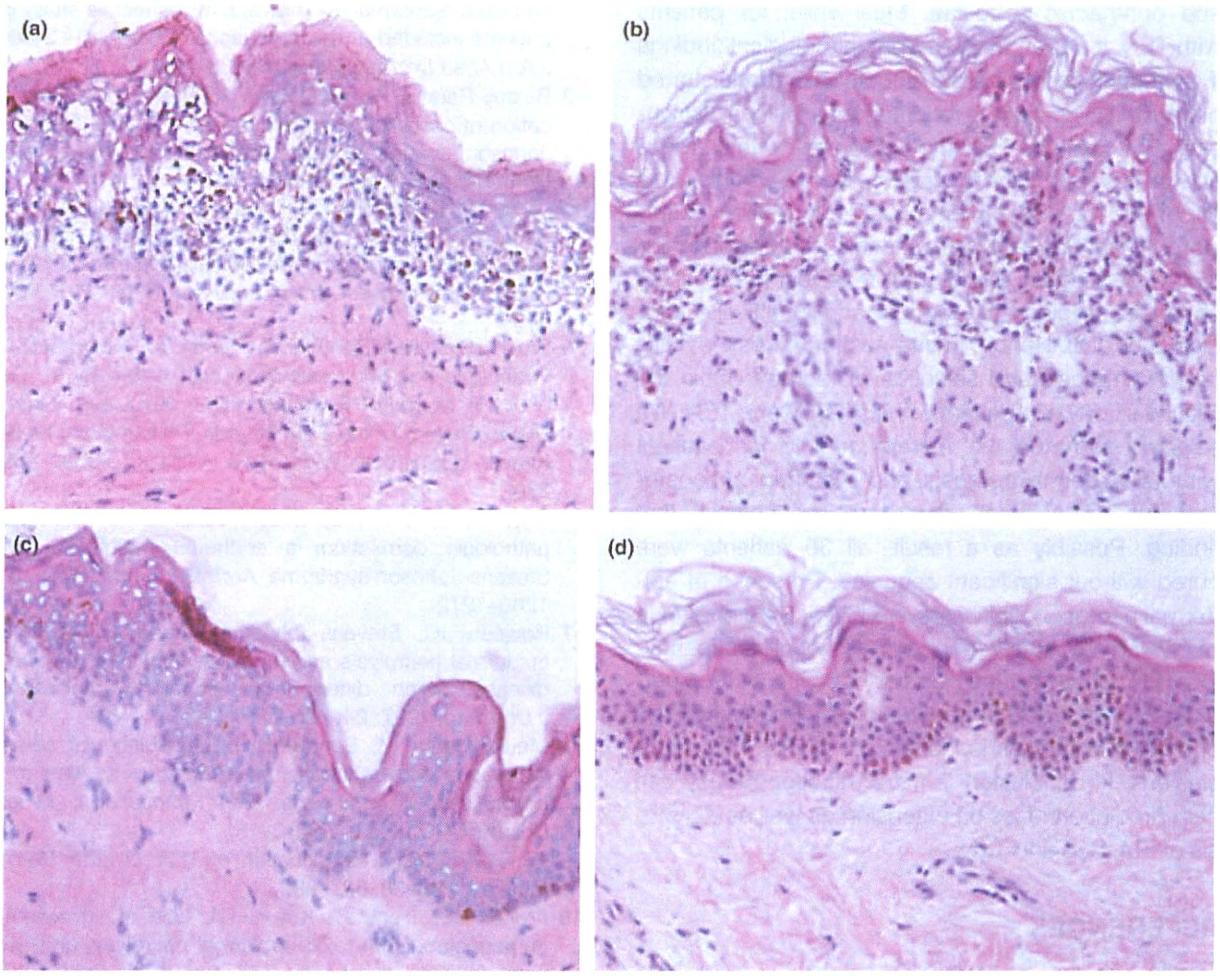

Figure 2. Histopathological findings of case 29. (a) Frozen sections from a lesion. (b) Permanent specimen from a lesion. Exocytosis of lymphocytes and epidermal necrosis are noted. (c) Frozen section of unaffected skin. (d) Permanent specimen from unaffected skin. No overt findings suggestive of graft-versus-host reaction (hematoxylin–eosin, original magnification ×400).

Table 2 Final diagnosis and histopathological findings

Final diagnosis	No. of patients	Epidermal necrosis (%)	GVHR-like findings in the epidermis (%)
TEN	1	1 (100)	1 (100)
SJS–TEN	1	1 (100)	1 (100)
SJS	4	4 (100)	0 (0)
EM	29	3 (10.3)	0 (0)
Major	8	1	0
Total	35	9 (25.7)	2 (5.7)

disease.[3,7,8] They are classified by skin detachment of body surface area as described above. Hence, if a patient is diagnosed as SJS, we consider the potential to exhibit a more aggressive clinical behavior, TEN. Our study suggested that GVHR-like findings in specimens from non-affected sites means greater extension of the lesion.[9] If that finding is seen in a SJS patient, he/she has a good possibility of development into TEN. Therefore, it is important to make a diagnosis and to assess disease activity correctly. Although initial diagnosis was correct in the majority of cases, two (33%) of six patients with SJS or TEN were misdiagnosed initially. We believe that frozen-section diagnosis is helpful for such cases.

Treatment of SJS and TEN, in particular therapeutic effect of i.v. immunoglobulin (IVIG), is subjective.[10,11] Our view is that systemic corticosteroid plus IVIG therapy is effective in SJS to prevent lesion extension

and ophthalmic sequelae. Meanwhile, for patients with TEN, it depends upon ophthalmological findings if systemic corticosteroid should be administrated because it is ineffective for cutaneous lesions. Whichever, EM, SJS and TEN should be dealt with individually for patients' care management. In particular, it is important for SJS patients to predict lesion extension.[12] Although a frozen section is of less quality than a permanent section, it can reveal presence or absence of epidermal damage and GVHR-like findings (Figs 1,2). Hence, frozen-section biopsy is helpful for diagnosis and selection of therapy within the initial-visit day of a patient with EM, SJS and TEN. We selected symptomatic therapy mainly for patients without epidermal necrosis, and systemic corticosteroid plus IVIG was considered only for ones with that finding. Possibly as a result, all 35 patients were cured without significant sequelae. Presence of epidermal necrosis signifies severe EM or SJS; presence of GVHR may signify more aggressive clinical behavior, TEN. However, the number of cases with epidermal necrosis that changed the initial clinical diagnosis and GVHR changes is insufficient to draw firm conclusions. In conclusion, a frozen-section biopsy can help prediction of lesion extension as well as diagnosis of EM, SJS and TEN.

REFERENCES

1 Aihara M, Ikezawa Z. Clinical study of deceased cases of toxic epidermal necrolysis (TEN) in Japan; comparative study with surviving cases of TEN and with deceased cases of Stevens-Johnson syndrome. *Jpn J Dermatol* 1999; **109**: 1581–1590.

2 Schneck J, Fagot JP, Sekula P *et al.* Effects of treatments on the mortality of Stevens-Johnson syndrome and toxic epidermal necrolysis: a retrospective study on patients included in the prospective EuroSCAR Study. *J Am Acad Dermatol* 2008; **58**: 33–40.

3 Bastuji-Garin S, Rzany B, Stern RS *et al.* Clinical classification of cases of toxic epidermal necrolysis, Stevens-Johnson syndrome, and erythema multiforme. *Arch Dermatol* 1993; **129**: 92–96.

4 Assier H, Bastuji-Garin S, Revuz J *et al.* Erythema multiforme with mucous membrane involvement and Stevens-Johnson syndrome are clinically different disorders with distinct causes. *Arch Dermatol* 1995; **131**: 539–543.

5 Wu H, Brandling-Benett HA, Harrist TJ. Noninfectious vesiculobullous and vesiculopustular diseases. In: Elenitsas R, Murphy GF, Johnson B Jr, Xu X eds. *Lever's Histopathology of the Skin*, 9th edn. Philadelphia: Wolter Kluwer, Lippincott Williams & Wilkins, 2009; 268–270.

6 Cote B, Wechsler J, Bastuji-Garin S *et al.* Clinicopathologic correlation in erythema multiforme and Stevens-Johnson syndrome. *Arch Dermatol* 1995; **131**: 1268–1272.

7 Roujeau JC. Stevens-Johnson syndrome and toxic epidermal necrolysis are severity variants of the same disease which differs from erythema multiforme. *J Dermatol* 1997; **24**: 726–729.

8 Mockenhaupt M, Schöpf E. Epidemiology of severe cutaneous drug reactions. In: Kauppinen K, Alanko K, Hannuksela M *et al.* eds. *Skin Reactions to Drugs*. Boston: CRC Press, 1998; 3–15.

9 Iijima M. Clinical classification of TEN. *Rinsho Derma (Tokyo)* 1996; **38**: 887–892.

10 French LE, Trent JT, Kerdel FA. Use of intravenous immunoglobulin in toxic epidermal necrolysis and Stevens-Johnson syndrome: our current understanding. *Int Immunopharmacol* 2006; **6**: 543–549.

11 French LE. Toxic epidermal necrolysis and Stevens Johnson syndrome: our current understanding. *Allergol Int* 2006; **55**: 9–16.

12 Iijima M. Judicial judgment for severe adverse drug reaction (ADR). *Arerugi* 2007; **56**: 1341–1345.

Case and Review

Dermatology

Dermatology 2010;221:17–22
DOI: 10.1159/000290775

Received: July 30, 2009
Accepted after revision: February 15, 2010
Published online: April 21, 2010

Occupational Trichloroethylene Hypersensitivity Syndrome with Human Herpesvirus-6 and Cytomegalovirus Reactivation

Hideaki Watanabe[a] Mikiko Tohyama[c] Michihiro Kamijima[d, e] Tamie Nakajima[e]
Takemi Yoshida[b] Koji Hashimoto[c] Masafumi Iijima[a]

[a]Department of Dermatology, Showa University School of Medicine, and [b]Department of Biochemical Toxicology, School of Pharmaceutical Sciences, Showa University, Tokyo, [c]Department of Dermatology, Ehime University Graduate School of Medicine, Toon, [d]Department of Occupational and Environmental Health, Nagoya City University Graduate School of Medical Sciences, and [e]Department of Occupational and Environmental Health, Nagoya University Graduate School of Medicine, Nagoya, Japan

Key Words
Hypersensitivity syndrome · Trichloroethylene · Human herpesvirus-6 · Cytomegalovirus · Drug-induced hypersensitivity syndrome · Drug rash with eosinophilia and systemic symptoms

Abstract
Patients having a generalised rash with severe liver dysfunction associated with exposure to trichloroethylene (TCE) have been reported mainly in Asian countries. However, no case has been reported in Japan since the 1990s. Here, we describe a case of hypersensitivity syndrome (HS) caused by TCE in a 30-year-old Japanese man. The patient developed a rash, fever and liver dysfunction 21 days after he had been exposed to TCE at his workplace. Serum human herpesvirus (HHV)-6 and cytomegalovirus (CMV) DNA were detected 4 and 7 weeks, respectively, after the onset; the IgG antibody titres to HHV-6 and CMV were significantly elevated 6 and 9 weeks, respectively, after the onset. Patch testing was positive for the metabolites of TCE (i.e. trichloroethanol, trichloroacetic acid and chloral hydrate) but not for TCE itself; these results suggest that the TCE metabolites induced this disease. Human leucocyte antigen-B*1301, which has been reported to be strongly associated with TCE-induced HS, was identified in this patient. In addition, the clinical findings, laboratory data and period of virus reactivation after onset were quite similar to those of drug-induced hypersensitivity syndrome (DIHS). We also review TCE-induced HS from the viewpoint of the similarity to DIHS in this article.

Introduction

Trichloroethylene (TCE) is a chlorinated solvent that is used to remove grease from metal parts or lenses and as an intermediate in the synthesis of other chemicals [1, 2]. Given its non-combustibility, low cost and low ozone depletion potential, it is still used as an industrial solvent [1].

A close link between occupational exposure to solvents, mostly TCE, and severe skin disorders, such as Stevens-Johnson syndrome, toxic epidermal necrolysis and hypersensitivity syndrome (HS), has been suggested [1]. Recently, the number of patients suffering from TCE-related severe skin disorders has been increasing in Asia, especially in the Philippines, Singapore, Taiwan and China [1]. Moreover, a reactivation of human herpesvirus (HHV)-6, the causative virus of exanthema subitum, has been demonstrated in such patients [3]. Recently, we observed a patient who developed a severe generalised rash with liver dysfunction, associated with the reactivation of HHV-6 and cytomegalovirus (CMV), after exposure to TCE. In addition, the characteristics of this patient, including the clinical findings and period of reactivation of these two viruses after onset, closely resembled those of drug-induced hypersensitivity syndrome (DIHS) [4–7], also referred to as drug rash with eosinophilia and systemic symptoms (DRESS) [8, 9]. This is the first report describing the reactivation of both HHV-6 and CMV in HS caused by TCE.

Case Report

A 30-year-old Japanese man with a history of atopic dermatitis from infancy was employed by a silicone manufacturer on August 25, 2004. On September 15, he noticed itching and a maculopapular eruption on his extremities. He also had a fever

KARGER

Fax +41 61 306 12 34
E-Mail karger@karger.ch
www.karger.com

1018–8665/10/2211–0017$26.00/0

Accessible online at:
www.karger.com/drm

Hideaki Watanabe, MD
Department of Dermatology, Showa University School of Medicine
1-5-8 Hatanodai, Shinagawa-ku
Tokyo 142-8666 (Japan)
Tel. +81 3 3784 8556, Fax +81 3 3784 8364, E-Mail hwatanabe@med.showa-u.ac.jp

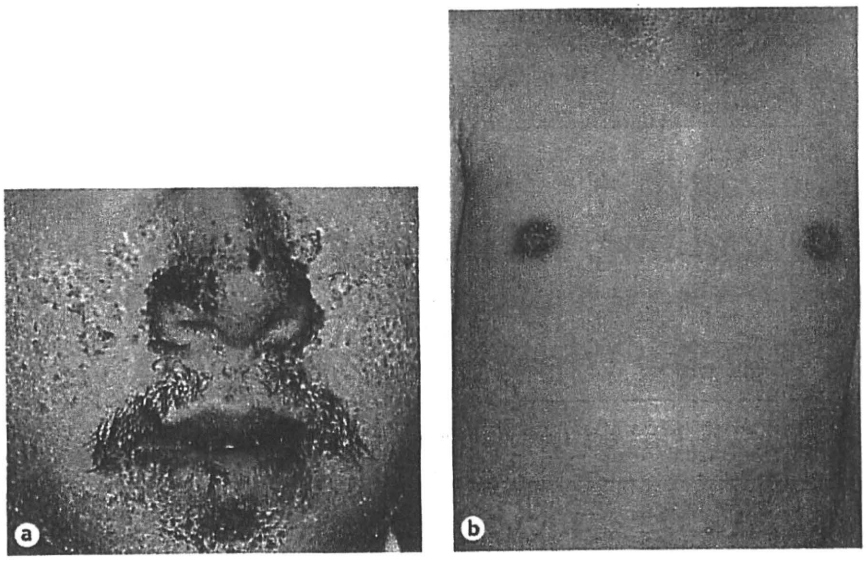

Fig. 1. Clinical examination on admission. **a** Oedema and erythema with scaling were observed on the face. Crusts were seen on the wings of the nose and around the lips. **b** Diffuse erythematous rash on the trunk.

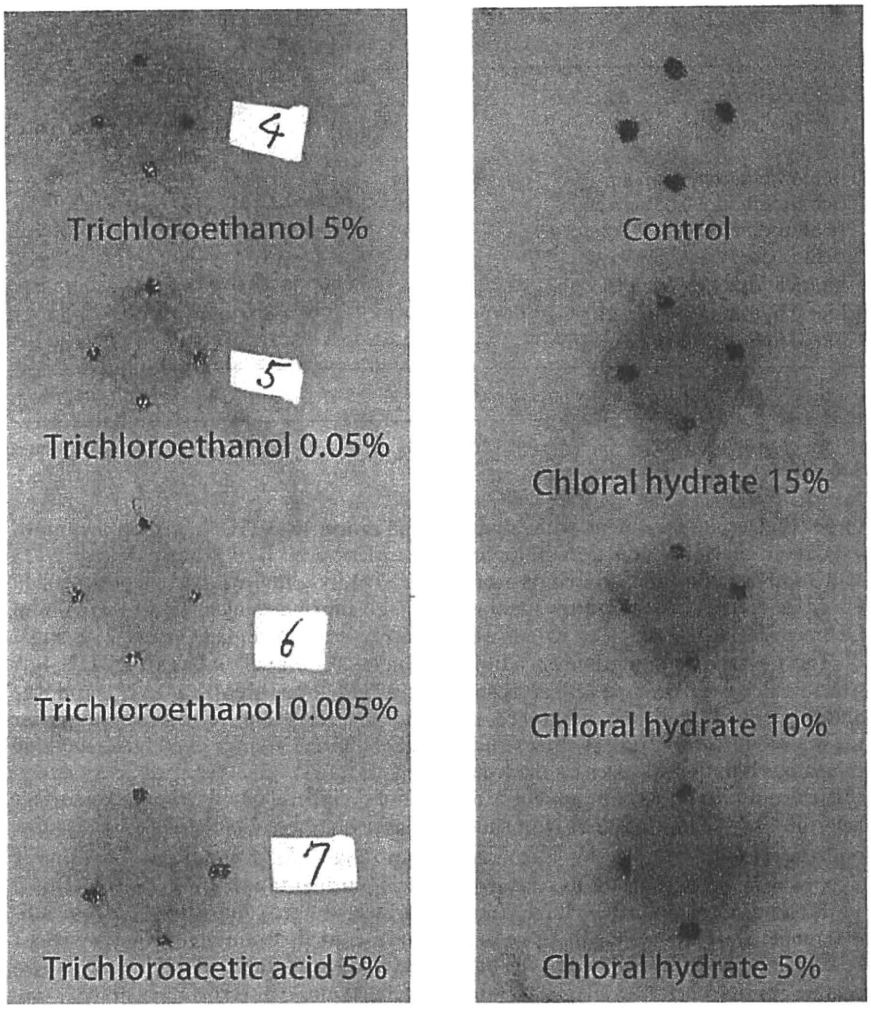

Fig. 2. Patch testing. Positive reactions (++) according to the ICDRG scoring system were observed for trichloroethanol (5, 0.05 and 0.005% in water), trichloroacetic acid (5% in water) and chloral hydrate (15, 10 and 5% in petrolatum). The reactions for TCE were negative at each concentration (25, 10 and 5% in olive oil).

Table 1. Immunoglobulin levels, viral DNA in serum and antibody titres after onset

Week	Date 2004–2005	HHV-6 IgM	HHV-6 IgG	HHV-6 DNA copies/ml[a]	CMV IgM	CMV IgG	CMV DNA copies/ml[a]	IgG mg/dl	IgA mg/dl	IgM mg/dl
3	Oct. 8	20	80	0	0.4	4.7	0	1,241	271	122
4	Oct. 14	n.d.	80	150,000	n.d.	n.d.	n.d.	n.d.	n.d.	n.d.
	Oct. 18	n.d.	5,120	0	n.d.	n.d.	0	n.d.	n.d.	n.d.
6	Oct. 21	20	10,240	0	0.47	5.0	0	n.d.	n.d.	n.d.
7	Oct. 25	n.d.	10,240	0	n.d.	n.d.	2.1×10^2	n.d.	n.d.	n.d.
	Nov. 1	n.d.	10,240	0	n.d.	n.d.	2.9×10^2	2,074	280	176
8	Nov. 8	20	10,240	0	0.52	71.4	3.6×10^2	2,342	323	228
9	Nov. 16	n.d.	n.d.	0	0.45	≥128	0	n.d.	n.d.	n.d.
38	July 27	n.d.	n.d.	n.d.	n.d.	n.d.	n.d.	2,063	392	164

Weeks are the weeks after onset. Normal ranges: IgG 800–1,750 mg/dl, IgA 100–450 mg/dl, IgM 45–300 mg/dl. n.d. = Not determined. [a] Detected in serum.

Table 2. Patch testing for TCE and its metabolites according to the ICDRG scoring system

	Reactions at 48 h	Reactions at 72 h
TCE 25% in o.o.	–	–
TCE 10% in o.o.	–	–
TCE 5% in o.o.	–	–
Trichloroethanol 5% in aq.	++	++
Trichloroethanol 0.05% in aq.	++	++
Trichloroethanol 0.005% in aq.	++	++
Trichloroacetic acid 5% in aq.	++	++
Chloral hydrate 15% in pet.	++	++
Chloral hydrate 10% in pet.	++	++
Chloral hydrate 5% in pet.	++	++

o.o. = Olive oil; aq. = water; pet. = petrolatum.

of 39°C. Despite treatment with topical steroid ointment and oral acetaminophen at a local hospital, his symptoms worsened. He was referred to our hospital on October 7.

The physical examination on admission revealed facial oedema with erythema and numerous scales and crusts around his nose and lips (fig. 1a). A diffuse erythematous eruption was seen on the trunk (fig. 1b) and extremities. The patient had a fever of 40.5°C and inguinal lymphadenopathy. He was negative for Nikolsky's sign. Laboratory investigations revealed a white blood cell count of $21.7 \cdot 10^9 \cdot l^{-1}$ (normal range: $3.5–9 \cdot 10^9 \cdot l^{-1}$), with 22% eosinophils and 5% atypical lymphocytes, aspartate aminotransferase 170 $IU \cdot l^{-1}$ (normal range: 10–30 $IU \cdot l^{-1}$), alanine aminotransferase 391 $IU \cdot l^{-1}$ (normal range: 5–25 $IU \cdot l^{-1}$), γ-glutamyl transpeptidase 245 $IU \cdot l^{-1}$ (normal range: 10–40 $IU \cdot l^{-1}$) and C-reactive protein 2.6 $mg \cdot dl^{-1}$ (normal range: <0.2 $mg \cdot dl^{-1}$). The serum IgG, IgA and IgM levels were 1,241, 271 and 122 $mg \cdot dl^{-1}$, respectively (normal range for IgG: 800–1,750 $mg \cdot dl^{-1}$; IgA: 100–450 $mg \cdot dl^{-1}$; IgM: 45–300 $mg \cdot dl^{-1}$). An analysis of peripheral blood lymphocyte surface markers showed 55.0% CD4+ T cells (normal range: 25–56%), and 26.6% CD8+ T cells (normal range: 17–44%). Hepatitis B surface antigen, hepatitis C virus antibody, human immunodeficiency virus-1 antibody and adult-T-cell-leukaemia-associated antigen were all negative. A skin biopsy from the thigh revealed hydropic degeneration of the epidermal basal cells and exocytosis of mononuclear cells in the epidermis. The upper dermis showed oedema and mild perivascular infiltration of mononuclear cells. At this time, we were unaware that he had been exposed to TCE. He was given systemic prednisolone 70 mg daily for 5 days, which proved effective. The dose was tapered over the next 12 days in line with the improvement in the clinical symptoms.

Four days after finishing the treatment with prednisolone (16 days after admission), however, the generalised erythematous lesions, fever, eosinophilia and liver dysfunction relapsed. The histological findings were similar to the results of the skin biopsy at admission. He was given systemic prednisolone 60 mg daily for 3 days, and the fever, rash and liver function parameters again improved markedly. The prednisolone was tapered off with the improved clinical symptoms. Given the onset, and because the clinical findings including the facial oedema, scales and crusts around the nose and lips, maculopapular eruptions and relapse during the course were quite similar to those of DIHS/DRESS [4–10], we examined whether certain herpesviruses had been reactivated. As shown in table 1, serum HHV-6 DNA measured by using real-time PCR, as described previously [4, 10], was detected 4 weeks after the onset (and only at this point). The HHV-6 IgG antibody titre determined by the indirect immunofluorescent antibody assay [4, 10] showed a 128-fold increase 6 weeks after onset in comparison with the titre on

Table 3. Results of patch testing for TCE and its metabolites in previous studies and our case

	TCE	Trichloro-ethanol	Trichloro-acetic acid	Chloral hydrate
Conde-Salazar et al. [18]	+			
Chae et al. [19]	+			
Nakayama et al. [11]	+	+	–	
Phoon et al. [20]	–			
Our case	–	+	+	+

Table 4. Diagnostic findings for HS due to TCE

Skin lesion	similar to DIHS (i.e. oedema of the face [1, 16], maculopapular rash [13, 26], erythroderma [26], exfoliative dermatitis [13, 16, 18, 26, 27], vesicles and blisters [16], pustules [18]); similar to EM (i.e. target lesion [20, 26, 27], blisters [26]); similar to SJS/TEN (i.e. severe mucous membrane involvement [2, 3, 20, 27], flat atypical target [3, 20, 26, 27], purpuric macules or blisters [3, 27])
Mucosal lesions	>38% [1–3, 20, 27]
Incidence	<1–13% of the exposed workers [1]
Onset of reaction	2–6 weeks [1, 3, 17, 20, 26–28]
Fever	73–86% [1–3, 16, 20, 26–29]
Lymphadenopathy	38–81% [1, 3, 16, 28, 29]
Eosinophilia	23% [1, 3, 16, 17]
Hepatitis	46–94% [1–3, 16, 17, 20, 27–29]
Other possibly involved organs	heart [26], lung [2], kidney [27], spleen [2], adrenal gland [1], larynx [1], brain [1]
Possible genetic factors	HLA-B*1301, HLA-B*44 [13]
Viral reactivation	HHV-6 [1, 3, 30], CMV
Airborne concentration	average 8-hour TCE exposure exceeding 135 mg/m^3 could increase risk of disease [1, 30]
Urinary metabolite	>50 mg/l trichloroacetic acid in the end-of-shift urine could increase risk [1, 26, 30]

EM = Erythema multiforme; SJS = Stevens-Johnson syndrome; TEN = toxic epidermal necrolysis.

admission. The anti-HHV-6 IgM titre did not change throughout the treatment period. In addition, serum CMV DNA measured using real-time PCR was detected 7 weeks after onset, and the anti-CMV IgG titre examined by an enzyme immunoassay was significantly elevated 9 weeks after onset. These findings demonstrate that both HHV-6 and CMV had been reactivated. The titres of antibodies against herpes simplex virus, varicella-zoster virus, HHV-7 and Epstein-Barr virus did not change throughout the clinical course. The patient was discharged from our hospital on November 5, 2004.

Two years after discharge, we became aware of a paper by Huang et al. [3] describing a generalised rash and liver dysfunction associated with HHV-6 reactivation due to TCE exposure. We asked the patient to visit our department, and after a detailed medical interview, we discovered that he had been exposed to TCE at his workplace. We then conducted patch testing for TCE and its metabolites, trichloroethanol, trichloroacetic acid and chloral hydrate, as previously reported [11, 12]. A positive reaction (++) according to the International Contact Dermatitis Research Group (ICDRG) scoring system was observed for trichloroethanol, trichloroacetic acid and chloral hydrate (table 2; fig. 2). A drug-induced lymphocyte stimulation test using chloral hydrate also showed significant elevation of the stimulation index (192 SI%, with the normal cutoff being 180 SI%). Human leucocyte antigen (HLA)-B*1301, which is reported to be strongly associated with TCE-induced HS [13], was present in this patient. Furthermore, the polymorphism of aldehyde dehydrogenase (ALDH), the major enzyme involved in TCE metabolism, was homozygous ALDH2 *1/*1 in this patient, which is also associated with TCE-induced HS [14]. The level of TCE and its metabolites in the patient's urine were not examined because he had left his job immediately after discharge from our hospital and had not been exposed to TCE subsequently. No other workers at the same plant had reported rashes or systemic complaints. Based on these findings, we made a final diagnosis of HS due to TCE.

Discussion

Generalised skin disorders due to TCE, which were originally described in an American textbook by Schwartz et al. [15] before the 1950s, began to increase after the mid-1990s in Asia [1]. So far, more than 200 cases of this disease have been reported in Asia [3], along with 5 cases from the USA [16, 17] and 1 from Spain [18]. Recent publications have documented fatal cases of HS [1–3]. In Japan, 5 reported cases of generalised skin disorders caused by TCE are known, but no case report has been published since the 1990s [1].